Fuel 195 (2017) 23–32

Contents lists available at ScienceDirect

Fuel

journal homepage: www.elsevier.com/locate/fuel

Full Length Article

Effect of different concentrations of O_2 under inert and CO_2 atmospheres on the swine manure combustion process

D. López-González [a], M.M. Parascanu [b], M. Fernandez-Lopez [a], M. Puig-Gamero [a], G. Soreanu [b], A. Avalos-Ramírez [c], J.L. Valverde [a], L. Sanchez-Silva [a,*]

[a] University of Castilla-La Mancha, Department of Chemical Engineering, Avda Camilo José Cela 12, Ciudad Real 13071, Spain
[b] Technical University 'Gheorghe Asachi' of Iasi, Department of Environmental Engineering and Management, 73 D. Mangeron Blvd, Iasi 700050, Romania
[c] Centre National en Électrochimie et en Technologies Environnementales, Québec, Canada

HIGHLIGHTS

- The study of the oxy-combustion of manure was carried out.
- Two different atmospheres were evaluated in this work: Ar/O_2 and CO_2/O_2.
- The kinetics of the process were computed by the Kissinger-Akahira-Sunose method.
- The gaseous products released during the process were evaluated by TGA-MS.

GRAPHICAL ABSTRACT

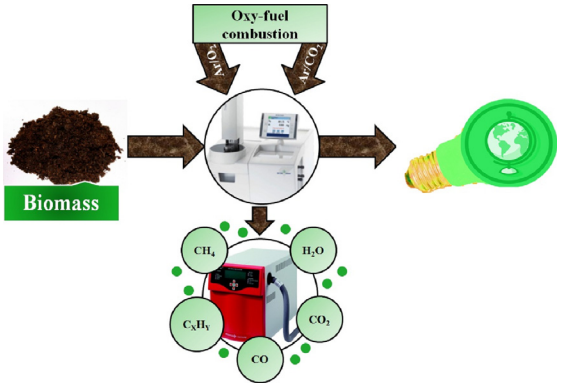

ARTICLE INFO

Article history:
Received 30 March 2016
Received in revised form 6 January 2017
Accepted 10 January 2017
Available online 18 January 2017

Keywords:
Combustion
TGA-MS
Manure
DSC

ABSTRACT

The oxy-fuel combustion of swine manure has been evaluated by thermogravimetric-mass spectrometric analysis. Manure samples showed a two-stage decomposition profile. The first stage is related to devolatilization of the sample and the second stage involved oxidation of the char formed *in situ*. Replacement of the inert carrier gas by CO_2 did not seem to affect the first stage. However, this change in carrier gas delayed the oxidation of the samples during the second stage. This finding is mainly attributed to the slower transfer of thermal energy to the fuels in CO_2/O_2 atmospheres. The increase in the oxygen partial pressure in the reaction medium had a marked effect on the oxidation stage by shifting the process to lower temperatures (from 514 to 478 °C and from 525 to 475 °C for Ar/O_2 and CO_2/O_2, respectively). The kinetics of the process were evaluated by the integral iso-conversional method of Kissinger–Akahira–Sunose (KAS). The two aforementioned stages were clearly identified as two regions of apparent activation energy were obtained. A similar profile was found for the gaseous products released in the process in both atmospheres, as evidenced by a distribution with two emission peaks, which is consistent with the two combustion regions. However, the formation of light products such as H_2, CO and CH_4 was favored on using high proportions of CO_2 (~80 vol.%).

* Corresponding author.
E-mail address: marialuz.sanchez@uclm.es (L. Sanchez-Silva).

http://dx.doi.org/10.1016/j.fuel.2017.01.041
0016-2361/

1. Introduction

The management of animal manure produced in the dairy, swine and poultry industries leads to losses of nitrogen (N), phosphorus (P) and carbon (C), which are emitted into the environment [1]. These losses have a direct impact on the environment and human health (climate change, terrestrial acidification, marine eutrophication and particulate matter formation) [1]. N is released through nitrate (NO_3^-) leaching, which contributes to eutrophication, and ammonia (NH_3) emissions. C contributes to greenhouse gas emissions (GHG), especially through the formation of CO_2 and CH_4, which are produced by manure fermentation. In this regard, livestock production accounts for an estimated 14% and 64% of world GHG and NH_3 emissions (78% of NH_3 emissions in Europe) [2]. The disposal of manure is responsible for a significant proportion of these figures. As a consequence, there is a need for the efficient management of manure produced in intensive livestock farming.

Manures from farming are commonly applied to land as fertilizers or they are processed by anaerobic digestion [3]. However, the manure produced in confined animal feeding operations (CAFO) is highly concentrated in certain regions and the levels produced exceed the requirements of the local farmland [4]. The number of studies on the conversion of manure to energy or to other added-value products by thermochemical conversion processes has increased in recent years [4–6]. Among the different thermochemical routes (pyrolysis, combustion and gasification), combustion is the most direct route for energy production. However, the use of manure alone in these types of processes is not currently viable due to the widespread nature of the locations where manure is produced. In any case, the high amounts in which they are produced (1500 million fresh tons of livestock waste and about 35 million dry tons of livestock waste is produced annually for the UE27 and the United States, respectively [7]) make manure interesting to be used in waste-to-energy processes.

The manure combustion process is usually carried out in an air atmosphere and this leads to several drawbacks, such as high exhaust heat loss and the difficulty in sequestering CO_2 from the exhaust gases due to the high nitrogen content of the effluent stream. Typically, only around 15% by volume of CO_2 is produced in a conventional coal-air combustion flue gas stream [8]. Oxy-fuel combustion has emerged as a plausible alternative to solve these problems through oxidation of the biomass in a pure flow of O_2. Under these conditions, carbon capture and sequestration (CCS) technologies can be easily integrated with oxy-combustion processes due to the higher concentration of CO_2 at the outlet. However, despite improvements in oxygen generation processes [9], the use of high concentrations of O_2 would lead to significantly increased costs and this compromises the final economic balance. In this respect, the use of a recycled flue gas (RFG) stream mainly composed of CO_2 and H_2O would reduce the operational costs and circumvent other operational problems such as high flame and char combustion temperatures by reducing the O_2 purity of the gas feedstream [10]. This influence is counteracted as a high RFG affects the economics of the process and it is critical to use the highest possible concentration of O_2 in the feed stream without compromising the stability of the boiler. From an environmental point of view, this technology also leads to lower NO_x emissions [11]. In this regard, the removal of N_2 from the feed stream eliminates the contribution of thermal NO_x formation. Additionally, conventional air-fired plants can be modified to work under oxy-fuel combustion conditions to yield similar performance levels [12] without requiring a higher capital investment than that already made in these plants [10].

The use of thermal analysis techniques coupled with analysis of the gas evolved provides an efficient tool for the evaluation of thermal processes [13,14]. However, the conditions employed differ greatly from those used in real combustors and other bench equipment such as drop tube furnaces and entrained flow reactors that simulate more closely the combustion conditions of industrial equipment. In any case, thermal analysis techniques have been widely used for solid fuel thermochemical conversion processes and are very valuable for comparison purposes and from a fundamental point of view [15,16]. The majority of the literature on these systems focuses on the study of oxy-fuel combustion processes with coal [8,11,17]. However, in recent years the use of biomass itself or in a blend for co-combustion has attracted increasing attention [18,19]. To the best of our knowledge, studies have not been reported in the literature that deal with the combustion of manure under different atmospheres (CO_2 and different O_2 concentrations).

The work described here concerns a thorough analysis of the oxy-fuel combustion process of manure. The optimum oxygen concentration, the kinetics of the process, the heat of combustion, the combustion characteristic factor (CCF) and the major contaminants in the effluent gas were evaluated in this study. Furthermore, the influence of replacing CO_2 in the feed stream was also evaluated.

2. Experimental section

2.1. Biomass samples

The samples used in this investigation were solid animal waste materials obtained from the province of Québec (Canada). Swine manure was selected for this study. Wet solids from swine manure containing 30% of dry matter were dried in a pilot-scale biodryer with a volume of 1 m^3. Biodrying is a bioprocess that removes water from waste using the heat generated by microorganisms during the degradation of organic matter. The biodryer used in this study was operated in semicontinous mode with a residence time of 7 days. The temperature profile of the bed varied from 25 to 65 °C depending on the height of the bed. The highest temperature was in the middle of the bed where the microorganisms showed the highest activity. At the exit of the biodryer, the dry matter content had increased up to 60–70% and the material had a calorific value of around 14 MJ/kg. Finally, the biomass sample was ground and sieved to an appropriate particle size (100–150 μm) and the sample was stored in a desiccator prior to use in the oxy-combustion processes.

2.2. Biomass characterization

The proximate analysis was performed according to the standard UNE-EN 14775:2010, UNE-EN 15148:2010 and UNE-EN 1474-2 guidelines for the determination of swine manure ash, volatile matter and moisture content, respectively. Fixed carbon was calculated by difference. The percentages of carbon, hydrogen, nitrogen, sulfur and oxygen (calculated by difference) in the sample were determined after complete combustion of the sample using a CHNS/O analyzer (model LECO CHNS-932) with sulfamethazine as the calibration standard.

Concerning heat of combustion, the highest heating value was determined according to the standard UNE-EN 164001:2005 method using a Parr 1356 calorimetric bomb unit. The analyses were repeated three times using benzoic acid to calibrate the equipment for determination of the heat capacity of the calorimeter with a confidence interval of ±150 cal/g.

2.3. Thermogravimetric analysis (TGA)

Oxy-combustion experiments were performed on a simultaneous thermogravimetric and differential scanning calorimeter

analyzer (TGA-DSC 1, Mettler-Toledo) coupled to a mass spectrometer (Thermostar-GSD 320/quadrupole mass analyzer, PFEIFFER VACCUUM) with an electron ionization voltage of 70 eV, which provides mass spectra up to 300 a.m.u. The interface between the two instruments was surrounded with heating wire in order to avoid condensation of the exhaust gases. Two different atmospheres were tested, namely CO_2/O_2 and Ar/O_2. Argon was preferred as the inert carrier gas rather than nitrogen because the nitrogen signal in the mass spectrometer interfered with key products such as CO ($m/z = 28$ for both compounds). The following partial pressures were tested for both atmospheres in order to evaluate the effect of O_2 concentration: 20, 40, 50, 60 and 80 vol.% O_2.

The temperature range studied was from room temperature up to 1000 °C at three different heating rates: 10, 20 and 30 °C/min. Preliminary experiments were performed according to Sanchez-Silva et al. [15] in order to minimise heat and mass transfer limitations. In this regard, a total gas flow of 100 NmL/min, a particle size range between 100 and 150 μm and an initial sample weight of 5 mg were used. The crucibles used were made of alumina and these had a total volume of 70 μL.

In order to identify ions with m/z values in the range 0–300, a preliminary broad scan was performed at a heating rate of 10 °C/min. Comparison of the peak areas between different samples was performed by applying the total pressure registered by the device as a normalization factor [20].

2.4. Kinetic analysis

In dynamic TGA experiments, the rate of conversion ($d\alpha/dt$) is the linear function of a temperature-dependent rate constant ($k(T)$) and the temperature-independent function of conversion ($f(\alpha)$) [21].

$$d\alpha/dt = k(T) \cdot f(\alpha) \tag{1}$$

where α is the degree of conversion (Eq. (2)) and k is the kinetic constant, which can be considered to follow an Arrhenius relationship (Eq. (3)):

$$\alpha = (m_o - m_t)/(m_o - m_f) \tag{2}$$

$$k = k_0 \cdot e^{-E_a/(R \cdot T)} \tag{3}$$

where m_o and m_t represent the mass at t = 0 and t = t, respectively, and m_f is the final mass of the sample, k_o is the pre-exponential factor, E_a is the activation energy, R is the universal gas constant and T is the absolute temperature (K).

Combination of Eqs. (1) and (3) yields:

$$d\alpha/dt = k_o \cdot e^{-E_a/R \cdot T} \cdot f(\alpha) \tag{4}$$

This equation provides a basis for differential kinetic methods [22]. Integration of Eq. (4) leads to Eq. (5).

$$g(\alpha) = \int_0^{\alpha} d\alpha/f(\alpha) = k_o \cdot \int_{t_o}^{t} e^{-E_a/RT} \cdot dt \tag{5}$$

where $g(\alpha)$ is the integral function of conversion.

By entering the linear heating rate program, the following equation is obtained:

$$\beta = dT/dt \tag{6}$$

$$g(\alpha) = \int_0^{\alpha} d\alpha/f(\alpha) = k_o/\beta \int_{T_o}^{T} e^{-E_a/RT} dT \tag{7}$$

2.4.1. Integral iso-conversional methods

All iso-conversional methods originate from the iso-conversional principle, which states that the reaction rate at a constant extent of conversion is only a function of temperature [22].

Integral iso-conversional methods involve the application of the iso-conversional principle to the integral equation (Eq. (5)). Eq. (5) does not have any analytical solution for any temperature program. For the commonly used constant heating rate program (Eq. (7)), the following approximation is widely accepted [22]:

$$\ln(\beta/T_{\alpha,i}^2) = B - C(E_a/RT_{\alpha,i}) \tag{8}$$

where B and C are parameters determined by the type of temperature integral approximation and $T_{\alpha,i}$ represents the temperature at which the extent of conversion α is reached under ith temperature program. In the work reported here, the approximation described by Kissinger–Akahira–Sunose (KAS) (B = 2 and C = 1) was used due to its high accuracy. The following expression was obtained [23]:

$$\ln(\beta/T_{\alpha,i}^2) = B - (E_a/RT_{\alpha,i}) \tag{9}$$

In iso-conversional methods a series of experimental runs is carried out at different heating rates [21]. Then, for a constant α, the plot of $\ln(\beta/T_{\alpha,i}^2)$ versus $1/T_{\alpha,i}$ for each value of α yields a straight line, the slope of which allows the apparent E_a to be evaluated. The term 'apparent E_a' is used due to the difficulty in determining intrinsic kinetic parameters for this kind of process, since each step is likely to be due to the decomposition of a mixture of compounds rather than an individual component. The use of 'apparent' parameters helps to differentiate them from intrinsic parameters, as explained by Vyazovkin et al. [22]. A region of apparent E_a is a region that has similar E_a values and it can be considered as a thermal decomposition step.

3. Results and discussion

3.1. Biomass characterization

The ultimate analysis, proximate analysis and calorific values for the swine manure sample are listed in Table 1. These characteristics determine the choice of conversion process and can have an influence on subsequent processing difficulties that may arise [24]. The swine manure sample had a relatively high C value (45 wt.%) and this is similar to those found in other types of terrestrial biomass. Furthermore, the levels of N and S, which could be converted into NO_x or SO_x upon oxidation, are considerably lower than those found for other types of biomass such as microalgae [25]. As far as the proximate analysis is concerned, it can be seen that the moisture content (M) is relatively low, which can be attributed to the bio-drying of the sample. A pre-drying step is required as the use of wet biomass, such as manure samples (>10 wt.% for air-dried manures), usually causes feeding problems. In this regard, a bio-drying pre-treatment was carried out as this is a viable and low-cost way to remove the excess moisture content. Heating of the biomass is caused by auto thermal heat generation due to microbial action on the waste material and, as a consequence, extra costs are not incurred in the process operation. Furthermore, the time required for biodrying is very short and the emission factors are also very short [26].

The fixed carbon (FC) and volatile matter (VM) contents make up almost 86 wt.% of the total composition, which make them good candidates for oxidation and gasification processes [24]. However, the amount of ash is high and this could cause different problems related to fouling, corrosion and slag formation. Finally, the High Heating Value (HHV) of the swine manure sample was 16.1 MJ/kg and this is similar to values found for swine (16.6 MJ/kg) [5] and chicken (18.3 MJ/kg) manure [3]. Furthermore, these values are quite similar to those determined for other types of biomass

Table 1
Characterization of the swine manure sample.

Ultimate analysis (wt.%) daf[a]					Proximate analysis (wt.%)[a]				HHV (MJ/kg)
C	H	N	S	O	M (%)	Ash (%)	VM (%)	FC (%)	
45.0	6.4	1.9	0.7	46.0	4.4	9.7	66.3	19.6	16.1

[a] daf = Dry and ash free basis; M = Moisture; VM = Volatile matter; FC = Fixed carbon; HHV = High heating value.

like lignocellulose (16–20 MJ/kg) [25] and microalgae (20–25 MJ/kg) [27,28]. Thus, characterization of the swine manure sample indicates that it has suitable properties for use in oxidation processes due to its high C, VM and FC contents in conjunction with its low moisture content. The use of manure as a fuel in its own right is not economically viable, mainly because its production is geographically disperse. Nevertheless, manure has similar properties to other types of biomass and it could be used as a co-combustion agent in coal or biomass-based power plants. This latter option is quite attractive since the usual high variability in the properties of manure can be circumvented by dilution with other solid fuels [29].

3.2. Thermal analysis

The thermal profiles for the oxy-combustion process of manure under inert (argon) and carbon dioxide atmospheres for an oxygen concentration of 20 vol.% at a heating rate of 20 °C/min are shown in Fig. 1. As described in previous works, the combustion process for biomass samples can be described by two main stages: devolatilization of the sample and oxidation of the resulting char [30]. The different shapes of the peaks are due to the decomposition of the main components of the biomass. The first peak is usually associated with the degradation of cellulose and hemicellulose tissue, whereas the second peak is related to the decomposition of more complex polymers like lignin [4]. The replacement of CO_2 by the inert gas did not seem to affect the thermal profile. As far as the first stage is concerned, significant changes were not observed on changing the atmosphere. The maximum decomposition peak for the Ar/O_2 atmosphere was obtained at 284 °C, with a weight loss rate of 0.52 wt.%/°C and a total weight loss of 48.5 wt.%. For the CO_2/O_2 atmosphere, the position of the peak was essentially the same, with a slightly lower rate (0.51 wt.%/°C) detected and total weight loss of 48.4 wt.%. This finding can be explained as follows: the devolatilization peak is highly associated with the removal of volatile matter from the biomass, which in turn is related to the activation energy and the temperature of the oxidant rather than to the reaction rate [31]. Thus, the devolatilization peak is more closely associated with thermal decomposition than the chemical reaction. On the other hand, more noticeable changes took place during the oxidation stage. For the CO_2/O_2 atmosphere, the sample decomposition was delayed from 514 °C to 525 °C. These findings are related to the higher specific heat capacity of carbon dioxide, which hinders the heat transfer rate and combustibility [32].

In relation to the DSC profiles (Fig. 1b), similar trends were observed with both atmospheres and this confirmed the presence of two different processes (i.e., two-step reactions). The second step was more exothermic than the first due to char oxidation [33]. As observed in the TGA-DTG profiles, there was a shift in the DSC peaks towards higher temperatures for the CO_2/O_2 atmosphere (the DSC peak for the CO_2/O_2 atmosphere was detected at 537 °C whereas the DSC peak for the Ar/O_2 one was observed at 517 °C). Furthermore, the peaks obtained on using the CO_2/O_2 atmosphere were taller than those observed for the Ar/O_2 atmosphere, a finding that could also be attributed to differences in the thermal properties of the two mixtures of gases.

The effect of the oxygen concentration is shown in Fig. 2. It can be observed that the temperature at which the main peak appeared for the devolatilization stage (275–278 °C ± 1 °C for both atmospheres) was not affected by the increased level of oxygen in the medium. The opposite effect was observed on considering the magnitude of the peak (from 0.49 to 0.58 ± 0.02 wt.%/°C for both atmospheres) and this is due to the fact that the volatiles are released quickly, as reported elsewhere [34]. In this regard, noticeable differences were not found in this stage for either atmosphere, which indicates that the temperature is the main driving force in the first step of the reaction. In contrast, the oxidation stage was clearly affected by the presence of oxygen, with the process shifted to lower temperatures. The main oxidation peak moved from 514 °C to 478 °C for the Ar/O_2 atmosphere and from 525 to 475 °C for the CO_2/O_2 atmosphere. These deviations are due to the higher level of oxidant, which influences the oxidation rate of the char. However, this effect was not observed at elevated oxygen concentrations [31]. The extent of the oxidation reaction, defined as the difference between the initial peak temperature and the burnout temperature, was more significant for the CO_2 atmosphere due to the slower transfer of thermal energy to the fuels.

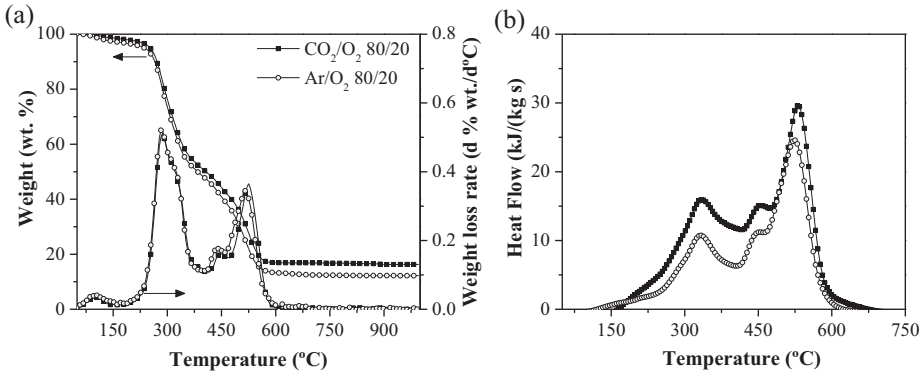

Fig. 1. Thermal analysis for the normal oxygen concentration combustion process under inert and CO_2 atmospheres. (a) Thermogravimetric (TGA) and derivative thermogravimetric (DTG) profiles and (b) differential scanning calorimetry (DSC) profiles.

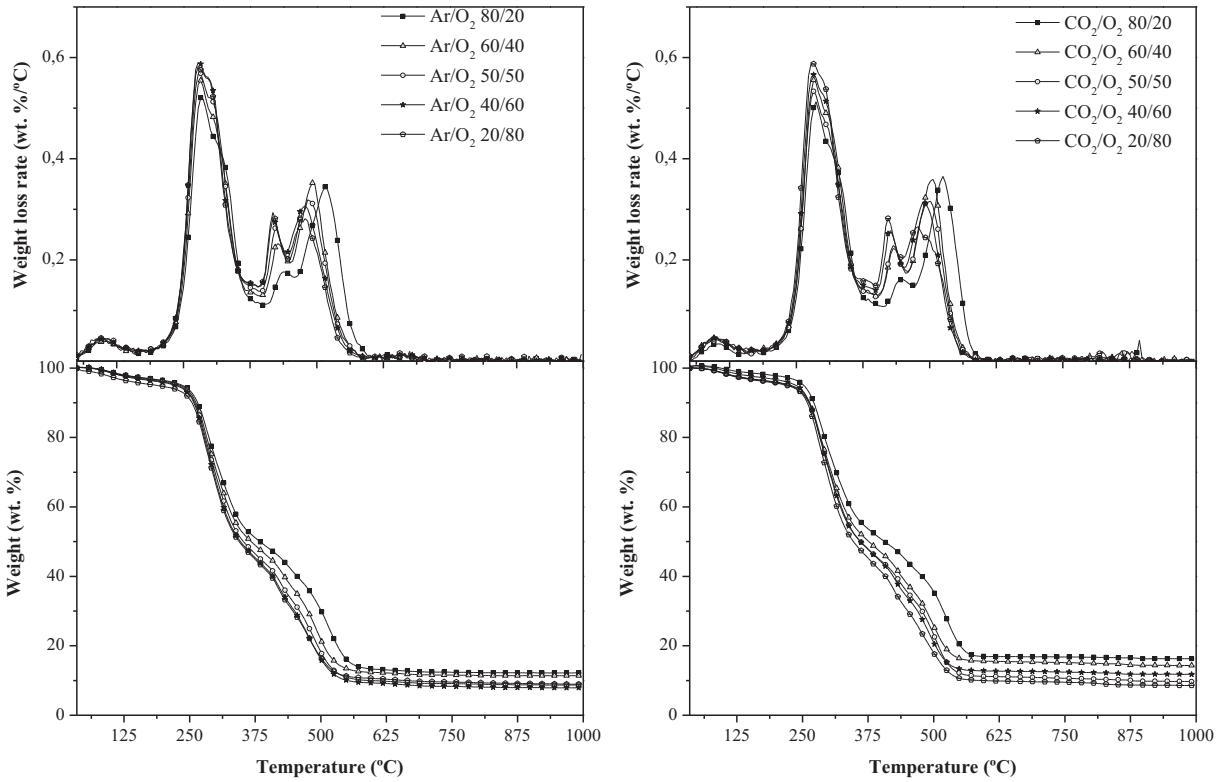

Fig. 2. Thermogravimetric (TGA) and derivative thermogravimetric (DTG) profiles for the oxy-combustion process for different oxygen concentrations under (a) inert and (b) CO_2 atmospheres.

3.3. Oxy-combustion efficiency

As discussed in the previous section, the efficiency of combustion can be defined by the second oxidation stage (i.e., the char oxidation stage). In this regard, comparison of the efficiency of the oxy-combustion process with respect to the partial pressure of oxygen was focused on this reaction region. Three different parameters were evaluated: the combustion characteristic factor (CCF), the maximum peak temperature (T_{pm}) and the heat of combustion determined by integration of the DSC peaks (ΔH_{comb}). The CCF estimates the efficiency of a process according to the maximum burning velocity ($(dw/dt)_{max}$ in wt.%/min), the average burning velocity ($(dw/dt)_{mean}$ in wt.%/min), the ignition temperature (T_i in K) and the burnout temperature (T_b). T_i is defined as the temperature at which a sudden weight loss is observed in the DTG curve. This parameter is calculated as the meeting point of the tangent line to the maximum weight loss rate and the tangent line to the point at which decomposition began. Finally, T_b is the temperature at which the combustion process finishes and further weight loss is not observed (temperature at which the weight loss rate is below 0.01 wt.%/°C). This factor has been used by several authors and is a good tool for comparison purposes [35,36]. The CCF can be expressed as:

$$CCF = \left(\frac{dw}{dt}\right)_{max} \cdot \left(\frac{dw}{dt}\right)_{mean} \Big/ T_i^2 \cdot T_b \quad (10)$$

The different parameters discussed above are depicted in Fig. 3. The variation in the maximum peak temperature with the oxygen concentration is depicted in Fig. 3a. The maximum peak temperature (T_{pm}) corresponds to a maximum weight loss region. In this regard, a lower T_{pm} value represents higher reactivity of the sample. The reactivity of swine manure is higher when Ar is used instead of CO_2. These results are consistent with those found elsewhere and are ascribed to the different specific heat capacity [31,37,38], mass diffusivity and thermal conductivity [32] of CO_2. Furthermore, for the Ar/O_2 atmosphere an inflection point was detected at an oxygen concentration of 60 vol.%. This observation indicates that higher oxygen concentrations did not lead to a further enhancement of the thermal process. In the case of the CO_2/O_2 atmosphere, an almost linear variation of the T_{pm} with oxygen concentration was observed. The evolution of both the combustion characteristic factor and the heat of combustion with oxygen concentration for Ar/O_2 experiments is represented in Fig. 3b. The former parameter increased linearly up to an oxygen concentration of 60 vol.% in a similar way to T_{pm}. However, the heat of combustion showed a different trend and in this case two regions were established. In the first region, for oxygen concentrations between 20 and 40 vol.%, the heat of combustion was relatively low. In the second region, for oxygen concentrations between 50 and 80 vol.%, an increase in the heat of combustion was observed. Regarding the CO_2/O_2 atmosphere (Fig. 3c), an inflection point was not found for the CCF parameter whereas the heat of combustion seemed to show a similar trend than that found in the Ar/O_2 experiments. However, in this case the lower heat of combustion values were extended up to an oxygen concentration of 50 vol.% whereas the higher values for this parameter were found at higher oxygen partial pressures (60–80 vol.% O_2).

In summary, on using an Ar atmosphere an optimum scenario was observed for oxygen concentrations between 50 and 60 vol.%. The presence of higher oxygen concentrations did not have a marked influence on the process. On using a CO_2 atmosphere, the maximum efficiency was found for the highest oxygen partial pressure used. As mentioned in previous sections, the maximum O_2 concentration must be controlled in terms of the flame temperature in order to keep it within the acceptable limits for the materials from which the boiler is constructed. Furthermore, control of the O_2 concentration will also reduce the cost of using a higher

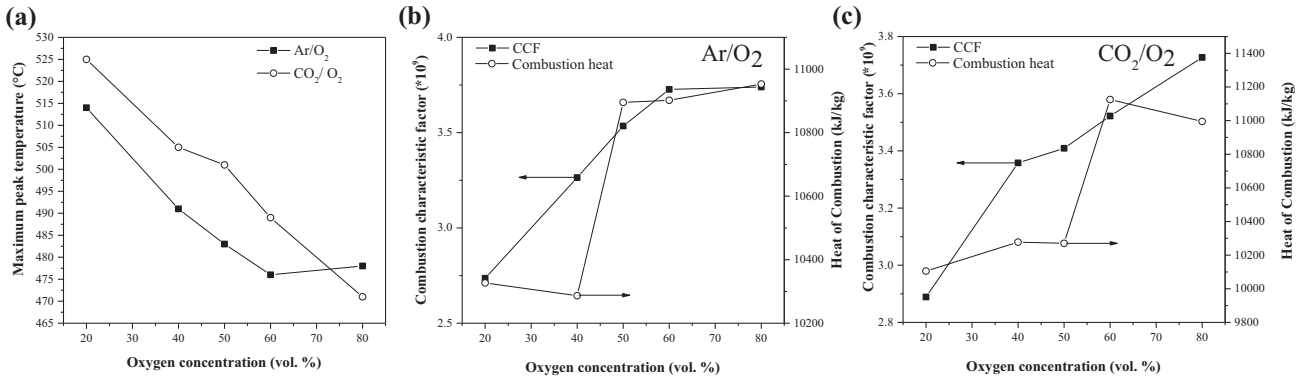

Fig. 3. Oxy-combustion efficiency in terms of: (a) maximum peak temperature, (b) combustion characteristic factor (CCF) and heat of combustion (ΔH_{comb}) for Ar/O_2 atmospheres and (c) combustion characteristic factor (CCF) and combustion heat (ΔH_{comb}) for CO_2/O_2.

amount of O_2 in the feed [39]. As pointed out by Ahn et al. [31], the optimized oxy-fuel conditions for existing power plants may be different depending on the fuel characteristics. Thus, customized studies for each type of biomass sample should be performed prior to their use in industrial applications.

3.4. Kinetic analysis

The linear plots obtained using the integral iso-conversional method of Kissinger–Akahira–Sunose (KAS) are shown in the Supplementary Information (Fig. S1). This method allows the acquisition of the apparent *Ea* of the sample under investigation from the slope of the iso-conversional plots, in which the derivatives of α and $\ln(\beta/T^2)$ are represented as a function of temperature. According to Eq. (9), a plot of $\ln(\beta/T^2)$ against $1/T$ should be a straight line. As can be seen in Fig. S1, the linear plots showed high correlation coefficients ranging from 0.9325 to 0.9999. Plots of the iso-conversional methods for the swine manure sample showed a general trend where the fitted lines were parallel. The slopes of the lines allow the estimation of the apparent activation energy of the dynamic combustion at various conversions [21]. As mentioned above, the use of iso-conversional methods allows the determination of the apparent *Ea* without any precise knowledge of the reaction mechanism [13].

The apparent *Ea* values as a function of α obtained by the KAS method are shown in Fig. 4. A significant variation in the apparent *Ea* with conversion indicates that the process is kinetically complex [22]. According to Babiński et al. [13], the dependence of *Ea* with the conversion rate in dynamic experiments is due to the change in the oxidation mechanism. However, it can be seen that the dependence of the apparent *Ea* on α can be separated into two distinct regions with similar apparent *Ea* values. The first region, in which iso-conversional *Ea* can be considered to be stable, corresponds to $0.1 < \alpha < 0.5$; the second region, where small variations of *Ea* were observed, is defined by $0.6 < \alpha < 0.8$. These two regions fit well with the two main stages of the oxidation processes discussed above. The low conversion range is associated with the devolatilization stage, whereas the high conversion range corre-

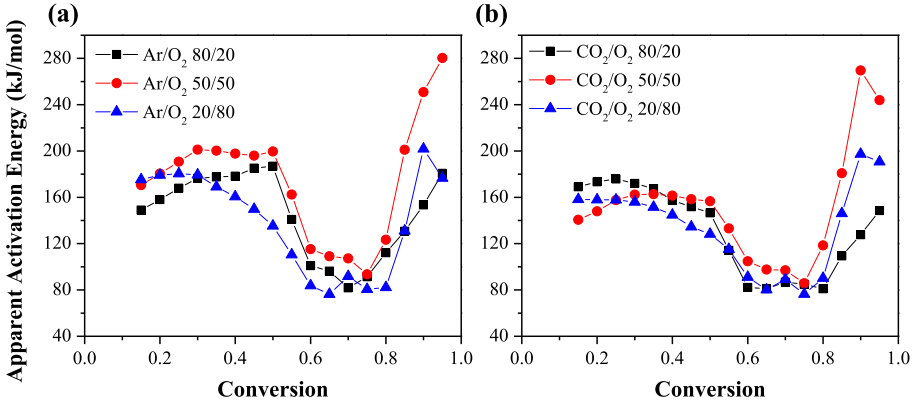

Fig. 4. Apparent activation energy as a function of the degree of conversion obtained by the KAS method for: (a) Ar/O_2 atmosphere and (b) CO_2/O_2 atmosphere.

Table 2
Apparent activation energy as a function of degree of conversion for the oxy-combustion process of swine manure in Ar and CO_2 atmospheres.

		Apparent *Ea* (kJ/mol)		
	α	20 vol.% O_2	50 vol.% O_2	80 vol.% O_2
Ar/O_2	0.1–0.5	180.51	195.75	170.07
	0.6–0.8	95.91	100.64	82.01
	α	20 vol.% O_2	50 vol.% O_2	80 vol.% O_2
CO_2/O_2	0.1–0.5	167.53	161.73	152.55
	0.6–0.8	87.96	96.03	84.08

Table 3
Comparison of combustion kinetics parameters for different types of manure samples.

Biomass	Ea (kJ/mol)		Method	Reference
	Step 1 (devolatilization)	Step 2 (char oxidation)		
Swine manure	198.7	124.2	Kissinger–Akahira–Sunose	[5]
Swine manure	–	107.0	Vyazovkin	[28]
Swine manure	–	119.6	Ozawa–Flynn–Wall	[28]
Bio-oil from swine manure	–	56	Single heating rate	[43]
Dairy manure	83.0	55.6	Single heating rate	[42]
Chicken litter	–	232	Friedman	[13]
Swine manure	180.5	95.9		Present study

sponds to the oxidation of the sample. The gap between the two conversion ranges probably corresponds to the intermediate peak observed in the DTG plots. These two regions are consistent with results reported in the literature [40,41]. The average apparent *Ea* values are summarized in Table 2 for each conversion range. The apparent *Ea* of the process did not seem to be very dependent on the amount of O_2 used in the medium. Thus, values of the same order of magnitude were found for Ar and CO_2/O_2 atmospheres but the value was slightly higher for the argon atmosphere. These values are consistent with those reported in the literature. In this regard, López et al. [42] found E_a values for the oxy-fuel combustion of corn and corn-rape blends in the range 132–190 kJ/mol for the devolatilization stage on using the Flynn–Wall–Ozawa (FWO) and Vyazovkin iso-conversional methods. Similarly, Chen et al. [32] found E_a average values in the range 134–242 kJ/mol for the oxy-fuel combustion of microalgae *Chlorella vulgaris* on using the FWO and KAS methods. However, comparisons between samples are complicated due to the wide range of operating conditions described in the literature (e.g., atmosphere, heating rate or kinetic approach). The values for the apparent activation energies for the two combustion regions for different types of manure samples are provided in Table 3. It can be seen that for different iso-conversional methods (e.g., Friedman, Kissinger–Akahira–Sunose or Flynn–Ozawa) the values obtained are very similar and small differences can be ascribed to different operating conditions and manure compositions. On the other hand, when single heating rate methods (i.e., Coats and Redfern) were used the experimental values obtained are underestimated (50–60 kJ/mol for the oxidation stage) [43,44]. In this regard, iso-conversional methods are considered to be more reliable since they are not dependent on the heating rate [21]. If we consider the two regions found, the apparent *Ea* values were higher for the devolatilization stage (low conversion values). This finding can be explained by the change in the combustion mechanism from chemical kinetic control (rate limiting) to diffusion-chemical kinetic control (fast step) [13]. On increasing the oxygen concentration in the medium, an increase at 50 vol.% O_2 and a decrease at 80 vol.% O_2 in the apparent *Ea* for both stages were observed. Werther and Ogada [45] observed an increase in the apparent *Ea* values and this suggests that the semi-coke structure expanded to give a higher grain size and the ash content increased with the increase in the final temperature.

The decrease in the apparent *Ea* at higher oxygen concentrations can be explained as follows. At high oxygen concentrations and temperatures, very little char remained and combustion was not a major event. This finding is in good agreement with previous studies reported by Fang et al. [34], who found a critical value for oxygen concentration of 65 vol.% for the oxy-fuel combustion of wood.

3.5. Analysis of evolved gas

The gaseous emissions produced during oxy-fuel combustion of the swine manure sample were evaluated by TGA-MS. The products were identified by a preliminary scan performed under the same conditions as the reaction but in the full range of ion to mass ratios (0–300). The most prominent ions were detected at (m/z) = 2, 15, 18, 26, 28, 29, 30, 44, 50, 58, 60 and 63 and these correspond to the following compounds: H_2, CH_4, H_2O, C_2H_2, CO, C_2H_6, $NO_x + CH_4N$ (primary amines) + light hydrocarbons, CO_2, CH_3Cl, C_3H_8N (amines), $C_2H_4O_2$ (oxygenated hydrocarbons) and $C_5H_3^+$ (aromatic indicator), respectively. Particular care must be taken when reporting some ions due to the fact that they could belong

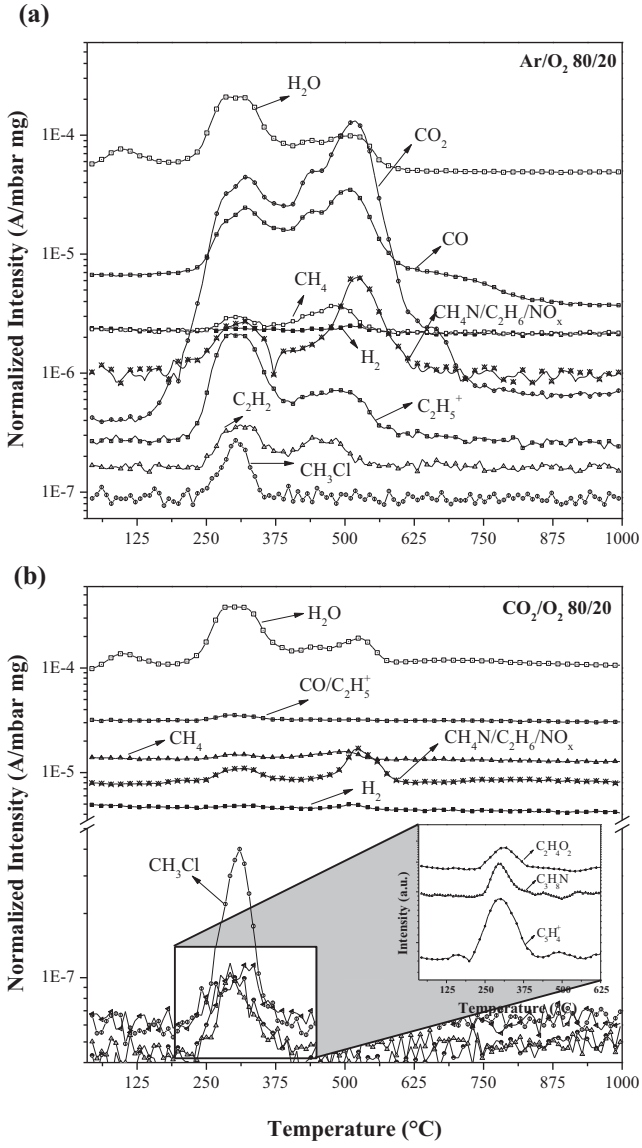

Fig. 5. Gas product distribution profile for the oxy-combustion of the swine manure sample for: (a) Ar/O_2 (80/20 vol.%) atmosphere and (b) CO_2/O_2 (80/20 vol.%) atmosphere.

to various compounds. For example, ions with m/z 30 are related to the evolution of different compounds such as NOx, primary amines and C_2H_6.

The gaseous product distribution for both types of atmospheres evaluated at 20 vol.% O_2 are shown in Fig. 5. A typical two-stage gas product distribution was found for the Ar/O_2 MS profile (Fig. 5a) [30,46]. The first stage corresponds to devolatilization of the sample, with the maximum intensity peak for most products observed at temperatures between 300 and 315 °C. Most of the volatiles were released during this stage and, as a consequence, a more diverse product distribution profile was found. As discussed above, decomposition processes were predominant in this temperature range. This fact, together with the prominent release of volatile matter, implies that oxygen did not reach the surface of the sample [13]. Thus, most of the compounds released in this stage, such as H_2, light hydrocarbons (CH_4, C_2H_2 and C_2H_6), CH_4N and chloride compounds (CH_3Cl), came from the thermal cracking of the sample. In a similar way, the H_2O detected in this stage was originated from the decomposition of glycosidic groups [47]. The second stage of the process corresponds to the oxidation zone. Maximum peaks were found in the temperature range 510–530 °C. In this stage the maximum peak was found for CO_2 and this indicates that direct oxidation of the char was the predominant reaction. The peak found in this stage at m/z = 30 was most likely related to the emission of NO_x due to the direct oxidation of the remaining N_2 in the char [30].

The gaseous product distribution in the case of CO_2/O_2 atmospheres is shown in Fig. 5b. The amount of products detected was lower than on using Ar/O_2 atmospheres because it was not possible to detect variations in CO_2. Nevertheless, a similar two-stage product distribution was found as described above and this is consistent with literature data [11,48]. The main gaseous product emitted was H_2O followed by CO, light hydrocarbons, amines, NO_x and H_2. Other products such as chloride compounds and aromatics were detected in much lower proportions.

The integrated peak areas for different concentrations of oxygen in the Ar/O_2 and CO_2/O_2 atmospheres are shown in Fig. 6. In this regard, the amount of CO_2 released might act as an indicator of

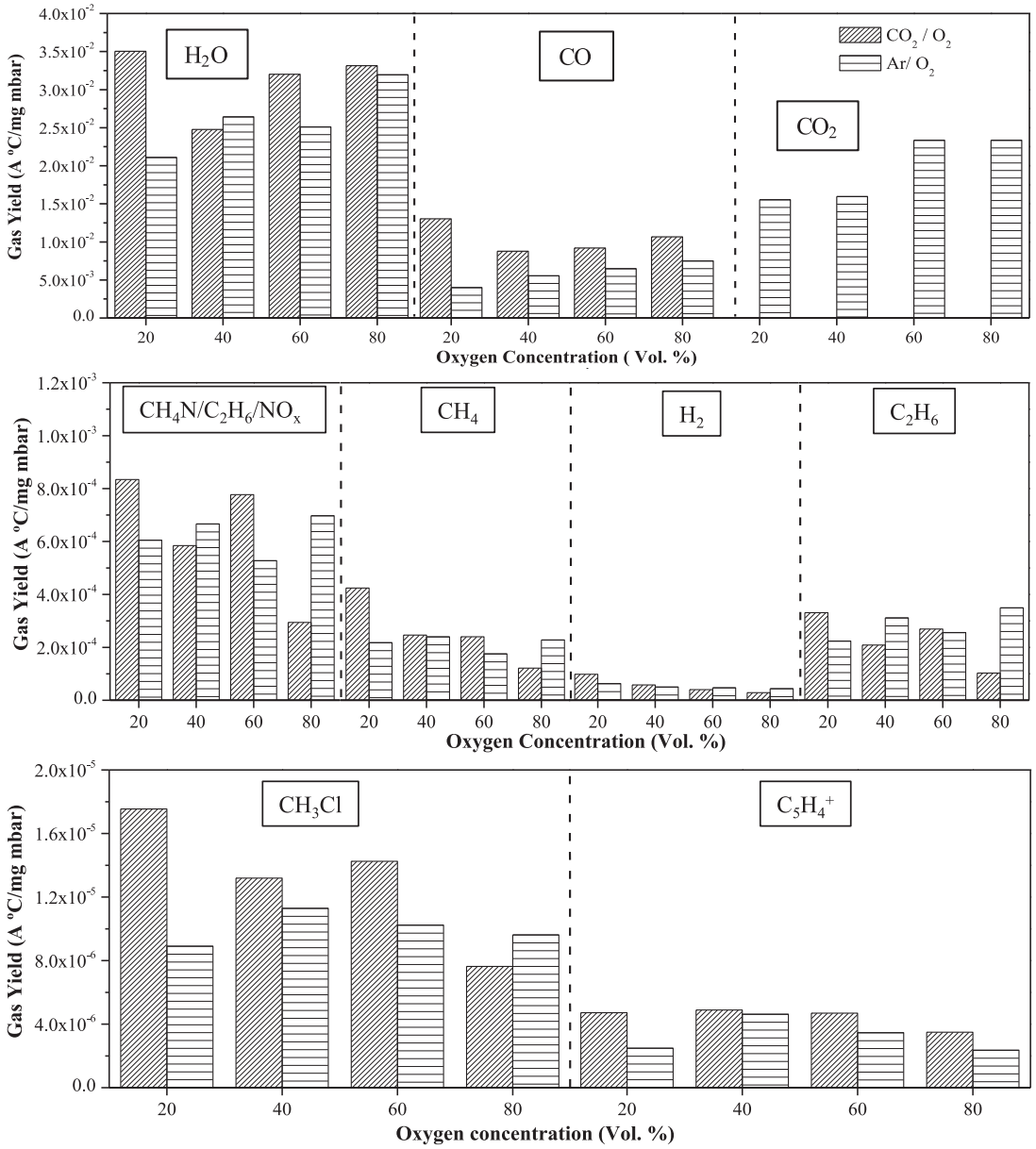

Fig. 6. Integrated peak areas for the oxy-combustion process of the swine manure sample in Ar/O_2 and CO_2/O_2 atmospheres against the amount of oxygen in the medium.

the combustion efficiency as it is the main product of the direct oxidation of char. Thus, a slow increase in CO_2 production with increasing amounts of O_2 in the medium from 20 to 40 vol.% was observed, with a maximum value obtained at 60 vol.% of O_2. The amount of CO_2 produced remained practically constant at 80 vol.%, which indicates that there is no significant enhancement in the process at high O_2 partial pressures. These results are in good agreement with those reported by Fang et al. [34], who found a maximum CO_2 production at oxygen levels between 50 and 60 vol.% for the oxy-fuel combustion of wood. The CO production increased almost linearly over the whole range of O_2 concentrations in the case of the Ar/O_2 atmosphere. However, for the CO_2/O_2 atmosphere, the maximum rate of CO production was obtained for the reaction mixture containing 80/20 vol.% of CO_2/O_2. The differences in CO emissions can be explained by considering the decomposition reactions (thermal cracking, partial oxidation and reforming reactions) of the manure sample that take place under CO_2/O_2 atmospheres [49]. However, at higher O_2 contents a drop in the level of CO production was observed and this can be explained by the occurrence of the Boudouard reaction ($CO_2 + C \leftrightarrow 2\ CO$) at low partial pressures of CO_2. Other typical gaseous products obtained from secondary reactions, such as H_2 or CH_4, showed similar trends, with maximum yields obtained at the highest CO_2 concentration tested (80 vol.%). However, for lower CO_2 concentrations the yields of these compounds were very similar to those observed for Ar/O_2 atmospheres. This result could indicate that secondary reactions (thermal cracking, Boudouard or reforming reactions) only took place at low O_2 concentrations and they were inhibited at higher concentrations where complete oxidation reactions are predominant. In general, the relative amounts of gaseous components were very similar for both types of atmospheres, which indicates that the use of CO_2 instead of Ar for oxy-combustion processes did not lead to a major change in the gaseous product distribution.

In summary, it can be concluded that swine manure samples could be a potential biomass feedstock for oxy-fuel combustion applications. This type of biomass has suitable characteristics such as high fixed carbon and volatile matter, low moisture and acceptably high heating values. On the other hand, the high ash content may require the inclusion of some pre-treatment process such as acid washing or co-firing of the manure with coal in order to solve these problems. The temperature needed to carry out the oxy-combustion process in the range 550–650 °C, which corresponds to the second oxidation zone. This temperature range is similar to those reported in the literature for other types of solid fuels such as lignocellulosic biomass and coal [34,48,49]. The amount of oxygen fed into the system could be in the range between 50 and 60 vol.%. However, the oxygen used in oxy-fuel combustion processes is very variable and it will change depending on the requirements of a particular system, as reviewed by Toftegaard et al. [39]. Concerning the gaseous emissions, SO_x emissions were not found although the emission of NO_x must be taken into consideration. However, further studies are required on conditions that more closely resemble those in real combustors such as drop tube furnaces and entrained flow reactors. In this regard, the kinetic data obtained in this work could be used for a preliminary prediction of the exhaust gas flows and the residence time of the manure in the combustors, as reported elsewhere [22,50,51].

4. Conclusions

The replacement of Ar by CO_2 as the carrier gas in oxy-combustion processes had a detrimental effect by delaying the oxidation of the sample. This fact was attributed to the higher specific heat capacity of carbon dioxide. An increase in the O_2 concentration in the medium enhances the oxidation of the sample up to a critical O_2 concentration, which indicates the existence of an optimum value where the combustion process cannot be enhanced further after a sufficient concentration of the reactant is present in the medium. This critical O_2 concentration was determined by employing different efficiency indicators (combustion characteristic factor, heat released during the combustion, maximum peak temperature and CO_2 production). In the case of Ar/O_2 atmospheres, an optimum O_2 concentration of 60 vol.% was found. However, on using CO_2 an optimum value was not found as this gas has a detrimental effect on the combustion process. Application of the Kissinger–Akahira–Sunose method showed that there were two different regions of apparent activation energy (E_a), namely a high apparent E_a (150–195 kJ/mol) for conversion values between 0.1 and 0.5 and a low apparent E_a (80–100 kJ/mol) for conversions between 0.6 and 0.8. The existence of two regions implied a change in the mechanism from chemical kinetic control to a diffusion-chemical kinetic control. The use of high concentrations of CO_2 (60–80 vol.%) in the reacting gas promoted the formation of secondary products such as H_2, CO and CH_4, which were ascribed to the existence of secondary reactions such as thermal cracking, reforming or Boudouard reactions. The main pollutants found were chloride compounds, NO_x and aromatic indicators, identified as CH_3Cl, $NO + NO_2$ and $C_5H_3^+$, respectively. The emission of these compounds took place during devolatilization of the sample between 200 and 400 °C except for NO_x, which was most likely released during the oxidation stage (400–600 °C).

Appendix A. Supplementary material

Supplementary data associated with this article can be found, in the online version, at http://dx.doi.org/10.1016/j.fuel.2017.01.041.

References

[1] De Vries JW, Hoogmoed WB, Groenestein CM, Schröder JJ, Sukkel W, De Boer IJM, et al. Integrated manure management to reduce environmental impact: I. Structured design of strategies. Agr Syst 2015;139:29–37.
[2] Loyon L, Burton CH, Misselbrook T, Webb J, Philippe FX, Aguilar M, et al. Best available technology for European livestock farms: availability, effectiveness and uptake. J Environ Manage 2016;166:1–11.
[3] Ekpo U, Ross AB, Camargo-Valero MA, Williams PT. A comparison of product yields and inorganic content in process streams following thermal hydrolysis and hydrothermal processing of microalgae, manure and digestate. Bioresour Technol 2016;200:951–60.
[4] Fernandez-Lopez M, Puig-Gamero M, Lopez-Gonzalez D, Avalos-Ramirez A, Valverde J, Sanchez-Silva L. Life cycle assessment of swine and dairy manure: pyrolysis and combustion processes. Bioresour Technol 2015;182:184–92.
[5] Sharara MA, Sadaka SS, Costello TA, VanDevender K, Carrier J, Popp M, et al. Combustion kinetics of swine manure and algal solids. J Therm Anal Calorim 2015;123:687–96.
[6] He BJ, Zhang Y, Funk TL, Riskowski GL, Yin Y. Thermochemical conversion of swine manure: an alternative process for waste treatment and renewable energy production. Trans ASAE 2000;43:1827–33.
[7] Choi HL, Sudiarto SIA, Renggaman A. Prediction of livestock manure and mixture higher heating value based on fundamental analysis. Fuel 2014;116:772–80.
[8] Gil MV, Riaza J, Álvarez L, Pevida C, Pis JJ, Rubiera F. Oxy-fuel combustion kinetics and morphology of coal chars obtained in N_2 and CO_2 atmospheres in an entrained flow reactor. Appl Energy 2012;91:67–74.
[9] Luo SY, Xiao B, Hu ZQ, Liu SM, Guan YW. Experimental study on oxygen-enriched combustion of biomass micro fuel. Energy 2009;34:1880–4.
[10] Glassman I. Combustion. 4th ed. Elsevier Science; 1997.
[11] Yuzbasi NS, Selçuk N. Air and oxy-fuel combustion characteristics of biomass/lignite blends in TGA-FTIR. Fuel Process Technol 2011;92:1101–8.
[12] Scheffknecht G, Al-Makhadmeh L, Schnell U, Maier J. Oxy-fuel coal combustion—a review of the current state-of-the-art. Int J Greenhouse Gas Control 2011;5(Suppl. 1):S16–35.
[13] Babiński P, Łabojko G, Kotyczka-Morańska M, Plis A. Kinetics of coal and char oxycombustion studied by TG-FTIR. J Therm Anal Calorim 2013;113:371–8.
[14] Zhang X, de Jong W, Preto F. Estimating kinetic parameters in TGA using B-spline smoothing and the Friedman method. Biomass Bioenergy 2009;33:1435–41.

[15] Sanchez-Silva L, López-González D, Garcia-Minguillan AM, Valverde JL. Pyrolysis, combustion and gasification characteristics of *Nannochloropsis gaditana* microalgae. Bioresour Technol 2013;130:321–31.
[16] López-González D, Fernandez-Lopez M, Valverde JL, Sanchez-Silva L. Comparison of the steam gasification performance of three species of microalgae by thermogravimetric-mass spectrometric analysis. Fuel 2014;134:1–10.
[17] Gil MV, Riaza J, Álvarez L, Pevida C, Pis JJ, Rubiera F. Kinetic models for the oxy-fuel combustion of coal and coal/biomass blend chars obtained in N_2 and CO_2 atmospheres. Energy 2012;48:510–8.
[18] Tan Y, Jia L, Wu Y. Some combustion characteristics of biomass and coal cofiring under oxy-fuel conditions in a pilot-scale circulating fluidized combustor. Energy Fuels 2013;27:7000–7.
[19] Lupiáñez C, Mayoral MC, Guedea I, Espatolero S, Díez LI, Laguarta S, et al. Effect of co-firing on emissions and deposition during fluidized bed oxy-combustion. Fuel 2016;184:261–8.
[20] Jones JM, Harding AW, Brown SD, Thomas KM. Detection of reactive intermediate nitrogen and sulfur species in the combustion of carbons that are models for coal chars. Carbon 1995;33:833–43.
[21] Chen C, Ma X, Liu K. Thermogravimetric analysis of microalgae combustion under different oxygen supply concentrations. Appl Energy 2011;88:3189–96.
[22] Vyazovkin S, Burnham AK, Criado JM, Pérez-Maqueda LA, Popescu C, Sbirrazzuoli N. ICTAC Kinetics Committee recommendations for performing kinetic computations on thermal analysis data. Thermochim Acta 2011;520:1–19.
[23] Akahira T, Sunose T. Method of determining activation deterioration constant of electrical insulating materials. Res Rep Chiba Inst Technol (Sci Technol) 1971;16:22–31.
[24] McKendry P. Energy production from biomass (Part 1): overview of biomass. Bioresour Technol 2002;83:37–46.
[25] López-González D, Puig-Gamero M, Acién FG, García-Cuadra F, Valverde JL, Sanchez-Silva L. Energetic, economic and environmental assessment of the pyrolysis and combustion of microalgae and their oils. Renew Sustain Energy Rev 2015;51:1752–70.
[26] Tom AP, Pawels R, Haridas A. Biodrying process: a sustainable technology for treatment of municipal solid waste with high moisture content. Waste Manage 2016;49:64–72.
[27] Kim SS, Ly HV, Kim J, Choi JH, Woo HC. Thermogravimetric characteristics and pyrolysis kinetics of Alga *Sagarssum* sp. biomass. Bioresour Technol 2013;139:242–8.
[28] Li D, Chen L, Zhang X, Ye N, Xing F. Pyrolytic characteristics and kinetic studies of three kinds of red algae. Biomass Bioenergy 2011;35:1765–72.
[29] Otero M, Sánchez ME, Gómez X. Co-firing of coal and manure biomass: a TG–MS approach. Bioresour Technol 2011;102:8304–9.
[30] López-González D, Fernandez-Lopez M, Valverde JL, Sanchez-Silva L. Kinetic analysis and thermal characterization of the microalgae combustion process by thermal analysis coupled to mass spectrometry. Appl Energy 2014;114:227–37.
[31] Ahn S, Choi G, Kim D. The effect of wood biomass blending with pulverized coal on combustion characteristics under oxy-fuel condition. Biomass Bioenergy 2014;71:144–54.
[32] Chen C, Lu Z, Ma X, Long J, Peng Y, Hu L, et al. Oxy-fuel combustion characteristics and kinetics of microalgae *Chlorella vulgaris* by thermogravimetric analysis. Bioresour Technol 2013;144:563–71.
[33] Kok MV, Özgür E. Thermal analysis and kinetics of biomass samples. Fuel Process Technol 2013;106:739–43.
[34] Fang MX, Shen DK, Li YX, Yu CJ, Luo ZY, Cen KF. Kinetic study on pyrolysis and combustion of wood under different oxygen concentrations by using TG-FTIR analysis. J Anal Appl Pyrol 2006;77:22–7.
[35] Wang S, Jiang XM, Han XX, Liu JG. Combustion characteristics of seaweed biomass. 1. Combustion characteristics of *Enteromorpha clathrata* and *Sargassum natans*. Energy Fuels 2009;23:5173–8.
[36] Jiang X, Huang X, Liu J, Zhang C. Effect of particle size on coal char-NO reaction. Front Energy 2011;5:221–8.
[37] Kiga T, Takano S, Kimura N, Omata K, Okawa M, Mori T, et al. Characteristics of pulverized-coal combustion in the system of oxygen/recycled flue gas combustion. Energy Convers Manage 1997;38:S129–34.
[38] Molina A, Shaddix CR. Ignition and devolatilization of pulverized bituminous coal particles during oxygen/carbon dioxide coal combustion. Prog Combust Inst 2007;31(II):1905–12.
[39] Toftegaard MB, Brix J, Jensen PA, Glarborg P, Jensen AD. Oxy-fuel combustion of solid fuels. Prog Energy Combust 2010;36:581–625.
[40] Moriana R, Zhang Y, Mischnick P, Li J, Ek M. Thermal degradation behavior and kinetic analysis of spruce glucomannan and its methylated derivatives. Carbohydr Polym 2014;106:60–70.
[41] López R, Fernández C, Cara J, Martínez O, Sánchez ME. Differences between combustion and oxy-combustion of corn and corn-rape blend using thermogravimetric analysis. Fuel Process Technol 2014;128:376–87.
[42] López R, Fernández C, Fierro J, Cara J, Martínez O, Sánchez ME. Oxy-combustion of corn, sunflower, rape and microalgae bioresidues and their blends from the perspective of thermogravimetric analysis. Energy 2014;74:845–54.
[43] Wu H, Hanna MA, Jones DD. Thermogravimetric characterization of dairy manure as pyrolysis and combustion feedstocks. Waste Manage Res 2012;30:1066–71.
[44] Wang L, Xiu S, Shahbazi A. Combustion characteristics of bio-oil from swine manure/crude glycerol co-liquefaction by thermogravimetric analysis technology. Energy Sources A: Recov Util Environ Effects 2016;38:2250–7.
[45] Werther J, Ogada T. Sewage sludge combustion. Prog Energy Combust 1999;25:55–116.
[46] López-González D, Fernandez-Lopez M, Valverde JL, Sanchez-Silva L. Thermogravimetric-mass spectrometric analysis on combustion of lignocellulosic biomass. Bioresour Technol 2013;143:562–74.
[47] Xie X, Goodell B, Zhang D, Nagle DC, Qian Y, Peterson ML, et al. Characterization of carbons derived from cellulose and lignin and their oxidative behavior. Bioresour Technol 2009;100:1797–802.
[48] Selcuk N, Yuzbasi NS. Combustion behaviour of Turkish lignite in O_2/N_2 and O_2/CO_2 mixtures by using TGA-FTIR. J Anal Appl Pyrol 2011;90:133–9.
[49] Li Q, Zhao C, Chen X, Wu W, Li Y. Comparison of pulverized coal combustion in air and in O_2/CO_2 mixtures by thermo-gravimetric analysis. J Anal Appl Pyrol 2009;85:521–8.
[50] López-González D, Fernandez-Lopez M, Valverde JL, Sanchez-Silva L. Pyrolysis of three different types of microalgae: kinetic and evolved gas analysis. Energy 2014;73:33–43.
[51] Conesa JA, Marcilla A, Font R. Kinetic model of the pyrolysis of polyethylene in a fluidized bed reactor. J Anal Appl Pyrol 1994;30:101–20.